Evaluating micellar liquid chromatographic methods on octadecyl particle-based and monolithic columns to predict the skin permeation of drug and cosmetic molecules

Grooten, Yasmine; Marcelis, Quinten; Mangelings, Debby; Vander Heyden, Yvan

Published in:
Journal of Chromatography. A

DOI:
10.1016/j.chroma.2021.462753

Publication date:
2022

Evaluating micellar liquid chromatographic methods on octadecyl particle-based and monolithic columns to predict the skin permeation of drug and cosmetic molecules

Yasmine Grooten[a], Quinten Marcelis[b], Debby Mangelings[a], Yvan Vander Heyden[a*]

[a] Vrije Universiteit Brussel (VUB), Department of Analytical Chemistry, Applied Chemometrics and Molecular Modelling, Laarbeeklaan 103, B-1090 Brussels, Belgium

[b] Vrije Universiteit Brussel (VUB), Department of In Vitro Toxicology and Dermato-Cosmetology, Laarbeeklaan 103, B-1090 Brussels, Belgium

*: Corresponding author

E-mail addresses: yasmine.grooten@vub.be (Y. Grooten), quinten.marcelis@vub.be (Q. Marcelis), debby.mangelings@vub.be (D. Mangelings), yvan.vander.heyden@vub.be (Y. Vander Heyden).

Abstract

A micellar liquid chromatographic method was developed to assist in the modelling of the skin permeability of pharmaceutical and cosmetic compounds. The composition of the mobile phase was determined by means of a two-factor central composite design, after which it was tested on both a particle-based and monolithic column. The latter provided the opportunity to increase the flow rate from 1 to 8 mL/min without reaching too high backpressures. The micellar conditions allowed analyzing a large test set of compounds with diverse characteristics with just one mobile-phase composition. The obtained experimental chromatographic descriptors besides two sets of theoretical molecular descriptors were used to model the skin permeability coefficient log K_p, applying multiple linear regression and partial least squares regression approaches. The micellar method on the monolithic column provided useful models with similar or even slightly better performance parameters than the method on the particle-based column. Furthermore, a much faster analysis can be achieved when applying a flow rate of 8 mL/min, making the micellar monolithic method ideal to estimate skin permeability.

Keywords

Skin permeability, micellar liquid chromatography, monolithic column, quantitative retention-activity relationship models, quantitative structure-activity relationship models

1. Introduction

The determination of skin permeability plays an important role in both drug development and risk assessment studies. The diffusion rate of a compound through the skin layers is then determined. The rate of transport is often indicated by the skin permeability coefficient K_p. However, determining this coefficient from *in-vivo* and *in-vitro* experiments often entails certain disadvantages, such as ethical remarks that can be made when using human or animal tests and the time-consuming characteristics of these approaches [1,2]. Moreover, alternative techniques are needed in the context of the replacement, reduction and refinement of animal experiments [2]. Different analytical methods have therefore been applied to predict the skin permeability of compounds, by using a chromatographic descriptor in a quantitative retention-activity relationship (QRAR) model [3–12].

Micellar liquid chromatography (MLC) is a type of reversed-phase liquid chromatography (RPLC), in which a surfactant is added to the mobile phase in a concentration exceeding the critical micelle concentration (CMC). In these conditions, micelles are formed in the mobile phase, resulting in a pseudophase which provides an extra dimension of interaction for a compound besides the stationary and mobile phase. Most often sodium dodecyl sulphate (SDS, anionic), cetyltrimethylammonium bromide (CTAB, cationic) or polyoxyethylene-(23)-lauryl ether (Brij-35, non-ionic) are used as surfactant, combined with different stationary phases, such as C18, C8 or cyanopropyl [13,14]. When Brij-35 is combined with a C18 column, this mode is also referred to as biopartitioning micellar chromatography (BMC) [15]. Furthermore, surfactant monomer adsorption to the stationary-phase surface also occurs, causing changes in its polarity (with non-ionic surfactants) or charge (with ionic surfactants), together with a shielding of the residual silanol groups. The addition of organic modifiers, mostly short-chain alcohols or acetonitrile, that form a hybrid micellar mobile phase, may accelerate the elution of compounds and enhance peak shapes. However, their concentration should be limited (often their fraction is in the range 3-15% v/v) given the negative effect on the formation of the micelles [16]. This low consumption of organic modifier contributes to the green character of MLC, together with a decrease in solvent costs. Furthermore, the use of a gradient can be avoided because both lipophilic and

hydrophilic compounds, covering a broad octanol-water partition coefficient (log *P*) range, can be determined with the same isocratic run [17].

Several studies have already applied a chromatographic descriptor obtained with MLC in QRAR models to predict skin permeability. Waters et al. [18] obtained a good model for the skin permeability based on the micelle-water partition coefficient (log P_{mw}, estimated from experimentally obtained retention factors) and the molecular weight. Their MLC method combined a cyanopropyl column with an SDS-based mobile phase, buffered at pH 5.5. Martínez-Pla et al. [19] applied a similar BMC approach and used the retention factor and melting point to model the skin permeability. Furthermore, this research group successfully predicted the pH effect on the skin permeability of compounds from BMC results [20]. A BMC system containing some acetonitrile in the mobile phase was used by Dobričić et al. [21] to predict the skin and corneal permeabilities of 17β-carboxamide steroids, using the obtained retention factors in artificial neural network (ANN), multiple linear regression (MLR) and partial least squares (PLS) quantitative structure-retention relationship (QSRR) models. After comparison, the PLS-QSRR model showed the best predictive properties.

Monolithic columns are composed of a single piece of porous material, characterized by a bimodal structure of macropores and mesopores [22,23]. Because of the highly porous characteristics of these columns, lower backpressures are acquired, which allows working at higher flow rates and achieving faster analyses (five to ten times faster than with particle-based columns) [24]. Detroyer et al. [25] compared the use of a monolithic and particle-based column, both with and without a micellar mobile phase based on SDS as surfactant, to predict log *P* (an indicator for membrane permeability). With this 'fast' micellar monolithic liquid chromatographic method the flow could be increased to 9 mL/min, maintaining a good correlation with membrane permeability. Furthermore, Lu et al. [26] have applied BMC successfully on a monolithic column to model the blood-brain barrier penetration, showing its potential as a fast and high-throughput method.

In previous research, the chromatographic retention on a C18 column showed little added value to skin permeability models relative to models with only theoretical descriptors [10]. Therefore, the aim of this study was to develop a micellar liquid chromatographic method on the same column type, and

additionally on a monolithic column, to improve the skin permeability prediction of pharmaceutical and cosmetic compounds. With MLC, a diverse set of compounds may be analyzed with one mobile-phase composition, due to the modification of the stationary phase by the surfactant monomers. Consequently, there is no need for extrapolation to a theoretical retention factor without organic modifier (log k_w) as is often the case in RPLC. From a two-factor central composite design approach, the best fraction of organic modifier (1-propanol) and concentration of surfactant (SDS) in the mobile phase were determined. The selected mobile phase was then used to screen a test set of 58 pharmaceutical and cosmetic compounds on both column types. The monolithic column was applied to obtain a fast and high-throughput MLC method. This approach has already been suitable to estimate intestinal absorption [25] and blood-brain barrier penetration [26], and will in this study be used for the prediction of skin permeability. Afterwards, the chromatographic data will be combined with molecular descriptors to model the skin permeability coefficient, applying MLR and PLS modelling approaches.

2. Materials and methods

2.1. *Reagents*

Methanol (MeOH, VWR Chemicals, Leuven, Belgium) and 1-propanol (Fisher Scientific, Loughborough, UK) were both HPLC grade. Sodium dodecyl sulfate (SDS), the anionic surfactant in the mobile phase, was purchased from Sigma Aldrich (Steinheim, Germany). Sodium acetate (Sigma Aldrich) was used to prepare a 0.05 M acetate buffer pH 5.5, adjusting the pH with 1 M hydrochloric acid (Fisher Scientific). The test set consisted of the following 58 compounds: 17α-hydroxyprogesterone, 2,4,6-trichlorophenol, 2,4-dichlorophenol, 2-amino-4-nitrophenol, 2-nitro-p-phenylenediamine, 4-amino-2-nitrophenol, acetylsalicylic acid, aminopyrine, atropine, benzyl alcohol, chloroxylenol, chlorpheniramine maleate, cortexolone, cortexone, corticosterone, cortisone, diclofenac, ephedrine.HCl, ethyl nicotinate, flurbiprofen, ibuprofen, indomethacin, ketoprofen, lidocaine, m-cresol, methyl nicotinate, m-nitrophenol, naproxen, o-chlorophenol, o-cresol**,** paracetamol, p-cresol, piroxicam, p-nitrophenol, p-phenylenediamine, prednisolone, progesterone, salicylic acid, testosterone, thymol, triamcinolone, triamcinolone acetonide (all Sigma Aldrich), amylobarbital and barbital (Bios Coutelier, Brussels, Belgium), benzoic acid, phenol, resorcinol, thiourea, β-naphthol (Merck, Darmstadt,

Germany), caffeine, methyl-4-hydroxybenzoate (Fluka, Neu-Ulm, Switzerland), hydrocortisone (Certa, Braine-l'Alleud, Belgium), estrone (Diosynth, Oss, The Netherlands), antipyrine, estriol, haloperidol, phenobarbitone and β-estradiol (gifts from unknown origin). The minimum purity of these compounds was 95%. Ultrapure water was provided by an Arium Pro UV system (Sartorius Stedim Biotech, Göttingen, Germany).

2.2. *Chromatographic conditions*

The HPLC system consisted of an L-7200 autosampler with a 100 µL loop, L-7100 pump, D-7000 interface and L-7400 UV detector from Merck-Hitachi (Tokyo, Japan). An external Igloo-Cil column oven (Amchro, Hattersheim, Germany) was used to keep the column temperature at 25°C. All compounds were analyzed at a wavelength of 220 nm. D-7000 HPLC System Manager software (Merck-Hitachi, 1994–2001, version 4.1) was used to process the obtained chromatographic data. The first disturbance of the baseline signal was used as the dead time. Buffers were vacuum-filtered through 0.20 µm membranes (Sartorius Stedim Biotech) and all mobile phases were degassed in an ultrasonic bath before use.

2.3. Two-factor central composite design to optimize the mobile phase

Mobile phases consisting of SDS in 0.05 M acetate buffer pH 5.5 (mimicking the pH of the skin) and 1-propanol were studied. A flow rate of 1.0 mL/min and an injection volume of 20 µL were applied. A smaller test set of 15 compounds, covering the log *P* range of the complete test set (-1.13 to 4.45), was selected: antipyrine, caffeine, cortexone, cortisone, diclofenac, ibuprofen, ketoprofen, lidocaine, methyl-4-hydroxybenzoate, paracetamol, prednisolone, progesterone, testosterone, thymol and triamcinolone. A two-factor central composite design requiring nine experiments was applied to optimize the concentration of the surfactant SDS (x_1) and the fraction of organic modifier 1-propanol (x_2) in the mobile phase. The range of the SDS concentration (0.01 - 0.15 M) was determined based on other research [27–29], keeping in mind the CMC of SDS. The experimental domain for 1-propanol was limited by the maximal amount that preserves the formation of the micelles (15% v/v 1-propanol) [30]. The two factors were explored on five levels ($-\alpha$, -1, 0, +1, $+\alpha$), of which the corresponding values can

be found in **Table 1**. For every mobile phase, the retention factor *k* of the 15 compounds was determined. For each compound second-order models were built to model the retention factor *k* as a function of the factors, according to the following equation:

$$k = \beta_0 + \beta_1 x_1 + \beta_2 x_2 + \beta_{12} x_1 x_2 + \beta_{11} x_1^2 + \beta_{22} x_2^2 \qquad \text{(Eq. 1)}$$

in which x_1 represents the concentration of SDS (in M), x_2 the percentage of 1-propanol and β_i the coefficients of the model. With this equation, the retention factors could be predicted for the entire experimental domain.

2.4. Particle-column experiments

An Xterra RP18 column (150 mm x 4.6 mm i.d., 5 µm) from Waters (Milford, MA, USA) was used for the particle-column experiments. A stock solution of 1.0 mg/mL of the standards was prepared in MeOH. The stock solutions were diluted 10 times with a 0.05 M SDS in 0.05 M acetate buffer pH 5.5 to obtain a final concentration of 0.1 mg/mL. The stock and working solutions were kept in the fridge until analysis (maximum duration of 2 months). A flow rate of 1 mL/min was applied and 10 µL of the standards was injected.

2.5. Monolithic-column experiments

A Chromolith Performance RP-18e column (100 mm x 4.6 mm i.d.) from Merck was used for the monolithic-column experiments. The flow was increased from 1 to 8 mL/min with steps of 1 mL/min (taking into account the maximal pressure of the column). An injection volume of 10 µL was applied. Standards of 1 mg/mL were prepared in MeOH, after which a dilution to 0.1 mg/mL was made in 0.08 M SDS in 0.05 M acetate buffer pH 5.5. Standard solutions were kept in the fridge until analysis.

2.6. Analysis of the entire test set

The test set of 58 compounds was analyzed with the mobile phase, consisting of SDS in 0.05 M acetate buffer pH 5.5 and 1-propanol, as organic modifier, in the quantities determined from the central composite design results. To assess the repeatability of injection, three compounds, caffeine (fast

eluting), m-nitrophenol (intermediate retention) and 2,4,6-trichlorophenol (slow eluting), were injected six times.

2.7. Data sources, software and data processing

Retention factors k were calculated as $(t_r - t_0)/t_0$, in which t_r stands for the retention time and t_0 for the dead time. The calculations and plots for the optimization of the mobile phase were made with m-files in MATLAB® 2014a (The Mathworks, Natick, MA, USA). The scatter plots were created with GraphPad Prism (GraphPad Software, San Diego, CA, USA, version 8.4.3).

The skin permeability coefficients, log K_p, were obtained from validated *in-vitro* tests reported in the literature [31–35]. Although it is not ideal to combine K_p values from different sources, it is difficult to avoid because of the lack of extended skin permeability data sets. A number of physicochemical, geometrical and topological descriptors, e.g. virtual log P, molecular weight and number of atoms, were calculated with Vega ZZ version 3.1.2.29 [36]. The melting point was derived from PubChem [37]. An additional set of molecular descriptors (a total of 1666 descriptors) was obtained from the E-Dragon software. These descriptors belong to different descriptor classes, such as constitutional indices, functional group counts, molecular properties, topological indices and atom-centred fragments [38,39]. (Nearly) constant variables and descriptor pairs with a high correlation ($r > 0.95$) were removed, keeping the variable which showed the highest correlation to the log K_p values.

The Vega ZZ software was used to build the MLR models applying the 'automatic linear regression' module. When a descriptor showed an r^2 below 0.10 with the skin permeability coefficient, it was not included in the model. Furthermore, highly correlated descriptors (variance inflation factor VIF > 5, with VIF = $1/(1-r^2)$) were not considered together in the MLR models. Models were built including one to seven descriptors. The software provided a ranking of the best models, from which the best model including the chromatographic descriptor was selected. An overview of these models is provided in the Supplementary material.

MATLAB® was used to compose stepwise MLR and PLS models. For the first modelling approach, forward selections are followed by backwards deletions of descriptors until a partial F-test determines

that the model is no longer improved by the addition or deletion of descriptors. For the best PLS model, the number of PLS factors is determined from the lowest root mean squared error of (leave-one-out) cross validation (RMSECV) value. For all models, the RMSECV and the root mean squared error of calibration (RMSEC) are calculated and used to validate the models, because lower values correspond to better models. The relative percentages of these parameters were calculated using the average log K_p values. The determination coefficient r^2 (between the log K_p(experimental) and log K_p(predicted)) was also used to assess the models.

3. Results and discussion

3.1. Selection of the mobile-phase composition

A small test set of 15 compounds was analyzed on the particle-based column according to the two-factor central composite design with nine different mobile-phase compositions, varying in concentration of SDS (surfactant) and percentage of 1-propanol (organic modifier) (see **Fig. 1**). The measured retention factors for each mobile phase can be found in **Table 2**. All compounds could be analyzed with every mobile-phase composition, even though the range of log *P* values was quite wide. It can be noticed that both an increase in SDS concentration as in fraction of 1-propanol led to an overall decrease in retention of the compounds. However, only MP 3 (0.03 M SDS + 12.8% v/v 1-propanol) and MP 6 (0.08 M SDS + 15% v/v 1-propanol) showed the same elution sequence, indicating that small partition changes can occur when changing the mobile-phase composition.

Building the quadratic polynomial models of Eq. 1 allowed predicting the response, i.e. the retention factors, for the entire experimental domain. **Fig. 2** shows an overlay plot of the predicted retention factors for caffeine (one of the earliest eluting compounds) and thymol (the last eluting compound). It is difficult to find an optimal mobile-phase composition, and we look for a compromise between the different responses. It is more important to indicate an area in the experimental domain in which the retention factor of caffeine is above 1 (to avoid co-elution with the injection peak) and the k value for thymol is reasonably low (to keep the analysis time within an acceptable time frame). Within this restricted area, the preference was given to a tested mobile phase, instead of interpolating in the domain. This resulted in three remaining mobile-phase compositions: MP 4 (0.08 M SDS without 1-propanol),

MP 5 (0.08 M SDS + 7.5% v/v 1-propanol) and MP 7 (0.13 M SDS + 2.2% v/v 1-propanol). Because the log *k* values of these three mobile phases are highly correlated (r between 0.988 – 0.998), they seem to contain similar information. Therefore, the mobile phase in the center of the domain (MP 5), consisting of 0.08 M SDS in 0.05 M acetate buffer pH 5.5 with 7.5% v/v 1-propanol, was chosen, since the surroundings of this point were explored in the design, in contrast to the mobile phases at the borders of the experimental domain.

3.2. *Analysis of the entire test set on the particle-based column*

After selection of the mobile-phase composition, the test set of 58 compounds was analyzed at the chosen conditions. The resulting retention factors ($k_{particle}$) can be found in **Table 3**, together with the skin permeability coefficients (log K_p), octanol-water partition coefficients (log P) and molecular weights (*MW*) of all compounds. The retention factors ranged between 0.45 and 140. However, the last eluting compound (haloperidol) showed an excessively high retention compared to the other analytes. Since haloperidol is completely positively ionized at pH 5.5, it is likely to interact extensively with the negatively charged SDS monomers adsorbed to the stationary phase. This compound was considered as an outlier for the modelling, leading to a new retention factor range of 0.45 – 38.9. The repeatability of injection was confirmed with a standard deviation below 0.1%.

When evaluating the relationship between the skin permeability coefficients, log K_p, and the retention factors, $k_{particle}$, a better correlation was obtained with the $k_{particle}$ values (r = 0.475) than with the log $k_{particle}$ values (r = 0.357). However, in both cases the retention factors on their own were insufficient to model the skin permeability. Therefore, two sets of molecular descriptors were considered to further improve the models, i.e. descriptors calculated with the Vega ZZ and E-Dragon software. First, MLR models were built with the molecular descriptors from the Vega ZZ software (see **Tables S1** and **S2** in the Supplementary material for an overview of the models containing $k_{particle}$ and log $k_{particle}$, respectively). When increasing the number of descriptors in these models, an improvement in the fit (lower RMSEC value) is noticed, which is also expected. Initially, the same trend is seen for the predictive capacities (RMSECV) of these models. However, after including a certain number of descriptors, the model becomes susceptible to overfitting, leading to an increase in the RMSECV values.

The best MLR model is therefore a compromise between fit and prediction, which in this case led to an optimal model with four descriptors, including the log $k_{particle}$, number of atoms, virtual log P and melting point (see Eq. 2 in **Table 4**). It should be noted that the best MLR model including $k_{particle}$ provided similar results.

When resorting to stepwise MLR modelling with E-Dragon descriptors, Eq. 3 (**Table 4**) was obtained with nine descriptors and the log $k_{particle}$.

$$\log K_p = -2.19(\pm0.44) - 0.36(\pm0.03)\ RDF020e + 0.51(\pm0.07)\ C\text{-}025 + 0.66(\pm0.12) \log k_{particle} + 1.88(\pm0.31)\ Lop + 0.25(\pm0.05)\ nCconj - 1.45(\pm0.30)\ GATS2p + 0.78(\pm0.20)\ Mor11m - 6.68(\pm2.24)\ RBF - 1.01(\pm0.30)\ G1p - 7.68(\pm3.36)\ JGI5 \quad \text{(Eq. 3)}$$

RMSEC = 0.329 (12.4%), RMSECV = 0.399 (15.0%), $r^2 = 0.93$, $n = 57$

This model showed a clear improvement compared to the MLR model with the Vega ZZ descriptors, both in terms of fit (r^2 and RMSEC) and predictive capabilities (RSMECV). The predicted log K_p values versus the experimental are plotted in **Fig. 3**, in which slightly more deviation is noticed for the lower log K_p values. The definition of the selected E-Dragon descriptors can be consulted in **Table S3** of the Supplementary material. The $k_{particle}$ values were not selected for the stepwise MLR model including the E-Dragon descriptors.

Furthermore, PLS models were constructed with both the log $k_{particle}$ and the Vega ZZ or E-Dragon descriptors. The best PLS models included the number of PLS factors resulting in the lowest RMSECV value. The Vega ZZ descriptor set led to a model with six PLS factors and somewhat similar performance parameters to the MLR model built with the same descriptor set (RMSEC = 0.694 or 26.1%, RMSECV = 0.813 or 30.5% and $r^2 = 0.69$). With the E-Dragon descriptor set, nine PLS factors led to the best model (RMSEC = 0.421 or 15.8%, RMSCEV = 0.730 or 27.4% and $r^2 = 0.89$). Although the RMSEC value for this model was better, the predictive properties (RMSECV) showed little improvement compared to the other PLS model. Furthermore, it is noticed that the influence of the chromatographic descriptor on the PLS models is rather low. Overall, the best model, which includes

the chromatographic descriptor from the particle-based column, was obtained applying stepwise MLR modelling on the E-Dragon descriptor set.

3.3. *Analysis of the entire test set on the monolithic column*

The mobile phase composition determined in 3.1. was also applied to analyze the test set on a monolithic column. The flow rate was increased from 1 to 8 mL/min with steps of 1 mL/min. With this flow rate increase, the pressure rises with about 22 bar per added mL/min. Therefore, the highest flow rate that could be applied, keeping in mind the maximal pressure of the column (200 bar), was reached at 8 mL/min. An overview of the individual retention factors at each flow rate can be consulted in **Table S4** of the Supplementary material. The average retention factors (k_m) at the different flow rates can be consulted in **Table 3**, together with their standard deviation. The average k_m values ranged between 0.02 and 43.58, with again haloperidol showing the highest value. This compound was again regarded as an outlier for the modelling, with the subsequent highest retention factor being 9.90 (chlorpheniramine maleate). Furthermore, acetylsalicylic acid and salicylic acid often showed little to no retention (k < 0.05), leading to their elimination from the modelling when using the log k values. The repeatability of injection was below 1.5%. The average relative standard deviation over the different flow rates was 8.70%. However, the correlation between the retention factors at 1 and 8 mL/min was 0.9998, indicating that there was no loss of information when increasing the flow rate. Therefore, the retention factors of the lowest and highest flow rates were used to model the skin permeability. In this way, it could be assessed whether similar models are obtained when increasing the flow rate.

When taking a look at the correlation between the retention factors obtained on the monolithic column and the skin permeability coefficients, it can be noticed that the retention factors at 1 mL/min, k_{m1}, and 8 mL/min, k_{m8}, show similar r values with the log K_p values (r = 0.458 and 0.447, respectively). Further, although the correlation between log K_p and log k_{m1} was less good (r = 0.380), a better correlation was seen with log k_{m8} (r = 0.470). Once more, these retention parameters without the use of theoretical descriptors were insufficient to model the skin permeability.

Theoretical descriptors were added besides the chromatographic to improve the models. An overview of the MLR models, including the retention factors from the lowest and highest flow rates (1 and 8 mL/min, respectively) and the Vega ZZ descriptors, ranging from one to seven descriptors, can be found in **Tables S5-S8** in the Supplementary material. When comparing these models, the best RMSECV is in both cases obtained by combining the log k_m with three Vega ZZ descriptors (Eqs. 4 and 5 in **Table 5**). For both models the number of atoms (*Atoms*), virtual log *P* and number of hydrogen bond donors (*HbDon*) were selected besides the chromatographic descriptor. The model including log k_{m8} (Eq. 5) was slightly better, but it should be noticed that only 55 compounds can be used, since salicylic acid and acetylsalicylic acid showed no retention ($k < 0.05$, of which no meaningful logarithmic value is obtained).

For the stepwise MLR models built with the E-Dragon descriptors, slightly better models were obtained when using the log *k* values instead of the *k* values (Eqs. 6-9 in **Table 5**). A number of common descriptors is found in these four models, i.e. *RDF020e*, *C-025* and *G1u*. The best model was again acquired using log k_{m8} (Eq. 9), showing very good results for the RMSEC, RMSECV and r^2 (see **Fig. 4**).

$$\log K_p = -3.33(\pm0.38) - 0.35(\pm0.03)\,RDF020e + 0.39(\pm0.07)\,C\text{-}025 + 0.80(\pm0.17)\log k_{m8} - 0.86(\pm0.30)\,G1u + 2.21(\pm0.35)\,Lop + 0.21(\pm0.07)\,EEig11d - 0.14(\pm0.06)\,ALOGPS\_logS + 0.56(\pm0.21)\,Mor11m - 13.25(\pm2.83)\,RBF + 1.67(\pm0.58)\,MATS2e - 0.61(\pm0.29)\,Mor18m \quad \text{(Eq. 9)}$$

RMSEC = 0.337 (12.6%), RMSECV = 0.412 (15.4%), $r^2 = 0.93$, $n = 55$

However, with 11 descriptors in total, this model was also the most complex. A description of the selected E-Dragon descriptors can be found in **Table S3** of the Supplementary material.

For the PLS modelling with the Vega ZZ descriptors, the retention factors k_m for a flow rate of 1 mL/min (RMSEC = 0.683 or 25.6%, RMSECV = 0.797 or 29.9% and $r^2 = 0.70$) and 8 mL/min (RMSEC = 0.683 or 25.6%, RMSECV = 0.807 or 30.3% and $r^2 = 0.70$) in both cases provided the best models with seven PLS factors. Thus, similar results were obtained at both flow rates. Using the E-Dragon descriptors, nine PLS factors were selected, leading to an improved model with log k_{m1} (RMSEC

317 = 0.421 or 15.8%, RMSECV = 0.730 or 27.4% and r^2 = 0.89), while at a flow of 8 mL/min k_{m8} (RMSEC
318 = 0.421 or 15.8%, RMSECV = 0.736 or 27.6% and r^2 = 0.89) gives the best PLS model. Although the
319 fit of these models clearly showed an improvement relative to the PLS model with the Vega ZZ
320 descriptors, the predictive capacities were similar as well as to the MLR models built with the Vega ZZ
321 descriptors. Again, it should be mentioned that the influence of the chromatographic descriptor is rather
322 low for these PLS models.

323 In conclusion, the models with the chromatographic descriptors from 1 and 8 mL/min showed
324 similar performance parameters, indicating that the same model quality can be obtained at increased
325 flow rate. Thus, a faster method can be used without a loss of information. The best model with a
326 chromatographic descriptor from the monolithic column was from the stepwise MLR approach and
327 includes log k_{m8} and E-Dragon descriptors.

328 3.4. *Comparison of the column types*

329 A test set of 58 compounds was analyzed on both a particle and a monolithic column, using the same
330 micellar mobile phase. On the particle column a flow rate of 1 mL/min was applied, while the monolithic
331 column allowed an increase of the flow from 1 to 8 mL/min (steps of 1 mL/min). When comparing the
332 retention factors on both columns (see **Fig. 5**), it can be noticed that the values on the particle column
333 were overall much higher than on the monolithic column. However, the correlation between these two
334 columns was lower than expected, i.e. r = 0.789 (without haloperidol), meaning that for some
335 compounds different elution mechanisms were at work.

336 In terms of analysis time, the elution of the most retained compound (haloperidol) on the monolithic
337 column (t_r = 56 min) only took about half the time of the analysis on the particle column (t_r = 126 min)
338 at the same flow rate (1 mL/min). It should be noted that shorter analysis times on the monolithic column
339 are already expected because of its shorter column length. When increasing the flow rate on the
340 monolithic column, the retention time of haloperidol further decreased to 7.75 min at a flow rate of
341 8 mL/min, which was almost seven times faster than the result at 1 mL/min on this column type. The
342 skin permeability models including the chromatographic descriptor from both column types are

compared. In addition, to explore the added value of these chromatographic descriptors, the obtained models were compared to models built with only theoretical descriptors in a previous study [10].

When comparing the models set up with the different retention descriptors, it can be noticed that the MLR models applying Vega ZZ descriptors showed similar parameters (Eqs. 2, 4 and 5). In all three cases, three molecular descriptors (besides log *k*) were selected for the best model, with the number of atoms and virtual log *P* as common descriptors. Using the particle-column retention in the model, the melting point was selected as fourth descriptor, while the number of hydrogen bond donors was selected for the monolithic column. When comparing these models to the best MLR models containing only Vega ZZ descriptors (four descriptors, RMSEC = 0.690 or 25.7%, RMSECV = 0.752 or 28.0% and r^2 = 0.69) [10], minimal improvement is noticed with the current models containing the retention information.

Further, the stepwise MLR models containing E-Dragon descriptors, besides log $k_{particle}$ (Eq. 3) or for the monolithic column either k_m or log k_m (Eqs. 6-9), were compared. A total of ten descriptors was used for the models including the results from the particle or the monolithic column at a flow of 1 mL/min, while at 8 mL/min on the monolithic column nine descriptors were selected when using k_{m8} and eleven with log k_{m8}. These stepwise MLR models showed very good values for RMSEC, RMSECV and r^2, with the best result coming from the analyses on the particle column. Furthermore, an improvement in the performance parameters is noticed in comparison to the best stepwise MLR model with only theoretical descriptors from an earlier study (stepwise MLR model with ten E-Dragon descriptors led to RMSEC = 0.378 or 14.1%, RMSECV = 0.452 or 16.8% and r^2 = 0.91) [10].

Finally, when considering the PLS models, those built with the Vega ZZ descriptors show similar performance parameters as the MLR models using the same descriptor set and this for both column types. An improvement in the RMSEC values was seen for the PLS models composed with the E-Dragon descriptors, for which the models from the particle-based and monolithic column (both at 1 and 8 mL/min) showed great similarities. This could be mainly attributed to the theoretical descriptors, because the influence of the chromatographic descriptor was rather low. In comparison to the PLS models built with only theoretical descriptors, more PLS factors were each time selected when the

retention descriptors from this study were added. The inclusion of the MLC retention results led to an improved fit compared to the PLS model based on only Vega ZZ descriptors, although no improvement in the predictive capabilities was observed (five PLS factors resulting in RMSEC = 0.757 or 28.2%, RMSECV = 0.807 or 30.0% and r^2 = 0.63). On the other hand, the PLS models based on E-Dragon descriptors showed a clear improvement when adding the chromatographic descriptors from MLC (six PLS factors, RMSEC = 0.674 or 25.1%, RMSECV = 0.860 or 32.0% and r^2 = 0.72) [10].

The overall best models were thus obtained with the stepwise MLR approach, applying E-Dragon descriptors. The models including log $k_{particle}$ (Eq. 3) or log k_{m8} (Eq. 9) show comparable results. Both models presented an added value of the chromatographic descriptor in comparison to the corresponding pure *in-silico* models, and are thus most suitable to apply in future skin permeability applications.

4. Conclusions

In this study, the retention obtained with micellar liquid chromatographic methods was used to model the skin permeability of pharmaceutical and cosmetic compounds. A limited test set was used to determine the optimal concentration of SDS and the percentage of 1-propanol in the mobile phase, using an experimental design approach. A mobile phase consisting of 0.08 M SDS in 0.05 M acetate buffer with 7.5% v/v 1-propanol was selected. These conditions were then applied to analyze a larger test set on two column types: a particle-based and a monolithic, the latter having the advantage of allowing an increase in flow rate to 8 mL/min without generating too high backpressures. Although there were some dissimilarities in retention between these two columns, the use of the retention factors (log k) provided similar models for the skin permeability. The addition of Vega ZZ descriptors provided the best MLR models with log P, number of atoms and melting point or number of hydrogen bond donors, i.e. descriptors that easily can be related to skin permeability processes. The stepwise MLR models containing E-Dragon descriptors were in this regard more abstract to interpret, but provided the best models. The PLS models built with E-Dragon descriptors also provided a good fit, but showed less good predictive abilities. Furthermore, these PLS models should be nuanced by the rather small importance of the chromatographic descriptor. Because both columns provided models with often similar quality, the monolithic column is preferred because of its faster operating conditions. Additionally, all models

were compared with skin permeability models containing only theoretical descriptors from a previous study, in which the same modelling approaches were applied. It was observed that the addition of the retention descriptor from the MLC methods provided improved models. In conclusion, the micellar method on the monolithic column offers a fast approach to effectively estimate the skin permeability of pharmaceutical and cosmetic compounds.

Acknowledgments

Y.G. is funded by a Ph.D. fellowship of the Research Foundation Flanders (FWO) [grant 11D3518N].

Conflict of Interest

The authors declare that they have no conflict of interest.

Tables

Table 1. The levels and factors varied in the two-factor central composite design.

Level	Factor	
	x_1 = concentration SDS (M)	x_2 = fraction 1-propanol (%)
-α	0.01	0
-1	0.03	2.2
0	0.08	7.5
+1	0.13	12.8
+α	0.15	15.0

Table 2. The measured retention factors *k* with the nine mobile-phase (MP) compositions of the experimental design. The SDS concentration (M) and fraction of 1-propanol (%) were specified for each mobile phase.

Compound	MP 1 0.01 M 7.5%	MP 2 0.03 M 2.2%	MP 3 0.03 M 12.8%	MP 4 0.08 M 0%	MP 5 0.08 M 7.5%	MP 6 0.08 M 15.0%	MP 7 0.13 M 2.2%	MP 8 0.13 M 12.8%	MP 9 0.15 M 7.5%
Antipyrine	1.81	2.91	0.87	2.89	1.43	1.15	1.72	0.68	1.23
Caffeine	1.16	1.69	0.59	2.00	1.09	0.90	1.32	0.50	1.03
Cortexone	66.2	26.6	15.4	11.9	10.5	8.14	6.80	4.57	6.08
Cortisone	15.7	12.5	4.58	6.30	4.93	3.35	3.58	2.09	3.11
Diclofenac	85.4	75.7	27.2	37.9	27.1	13.1	22.3	8.69	16.1
Ibuprofen	76.8	64.2	26.1	35.8	22.0	12.9	19.6	7.83	13.2
Ketoprofen	9.23	13.6	4.20	10.8	5.85	3.11	6.09	2.32	4.51
Lidocaine	134	57.8	28.7	25.1	18.1	13.4	13.3	6.92	9.74
Methyl-4-hydroxybenzoate	19.4	19.0	8.98	12.3	10.1	7.33	8.08	4.86	6.97
Paracetamol	1.19	1.31	0.70	1.44	1.08	1.05	1.13	0.59	1.02
Prednisolone	19.9	15.0	5.44	7.81	5.39	3.73	4.16	2.24	3.32
Progesterone	136	41.1	33.3	15.7	19.2	16.5	10.2	9.02	9.78
Testosterone	72.7	26.1	19.2	10.6	12.1	10.4	6.69	5.78	7.03
Thymol	196	105	57.8	47.9	39.7	30.1	28.8	16.5	22.7
Triamcinolone	8.10	7.54	2.84	3.83	3.53	2.42	2.47	1.52	2.41

414 **Table 3.** The octanol-water partition coefficients (log *P*), skin permeability coefficients (log K_p),
415 molecular weights (*MW*) and the retention factors on both the particle-based ($k_{particle}$) and monolithic
416 column ($\bar{k}_m$, average for the different flow rates, along with the standard deviation *s*).

Compound	**log *P*** [a]	***MW*** [a]	**log K_p** [b]	$k_{particle}$	$\bar{k}_m$ **(*s*)**
17α-Hydroxyprogesterone	1.84	330.46	-3.22	13.35	2.72 (0.09)
2,4,6-Trichlorophenol	3.94	197.45	-1.23	38.65	7.15 (0.21)
2,4-Dichlorophenol	3.18	163.00	-1.22	28.11	5.51 (0.15)
2-Amino-4-nitrophenol	1.39	154.12	-3.18	6.00	0.80 (0.04)
2-Nitro-p-phenylenediamine	0.78	153.14	-3.30	4.43	1.05 (0.04)
4-Amino-2-nitrophenol	1.22	154.12	-2.55	5.53	1.32 (0.05)
Acetylsalicylic acid	1.10	180.16	-2.14 [33]	0.46	0.02 (0.04)
Aminopyrine	1.57	231.29	-2.99	3.63	1.55 (0.06)
Amylobarbital	1.97	226.27	-2.64	11.51	3.42 (0.10)
Antipyrine	1.26	188.23	-4.18	1.46	0.66 (0.03)
Atropine	2.14	289.37	-5.07	11.47	4.29 (0.13)
Barbital	0.95	184.19	-3.96	2.24	0.55 (0.03)
Benzoic acid	1.24	122.12	-1.52	1.07	0.19 (0.03)
Benzyl alcohol	1.34	108.14	-2.22	3.71	1.11 (0.05)
Caffeine	-0.25	194.19	-2.80	1.08	0.48 (0.03)
Chloroxylenol	3.06	156.61	-1.23	28.81	6.11 (0.18)
Chlorpheniramine (maleate)	3.86	274.79	-2.66	23.33	9.90 (0.29)
Cortexolone	0.97	346.46	-4.12	8.39	1.81 (0.06)
Cortexone	1.92	330.46	-3.35	10.55	2.80 (0.10)
Corticosterone	0.82	346.46	-3.19	6.81	1.80 (0.07)
Cortisone	-0.12	360.44	-5.00	4.97	1.11 (0.04)
Diclofenac	4.45	296.15	-1.74	26.87	5.67 (0.22)
Ephedrine.HCl	1.73	165.23	-2.22	17.57	8.12 (0.21)
Estriol	2.30	288.38	-4.40	16.87	0.56 (0.04)
Estrone	3.18	270.37	-2.44	27.10	3.20 (0.11)
Ethyl nicotinate	1.35	151.16	-2.20	4.99	3.52 (0.09)
Flurbiprofen	3.88	244.26	-0.34	19.96	5.04 (0.19)
Haloperidol	3.75	375.86	-4.04 [34]	140.43	43.58 (1.23)
Hydrocortisone	0.01	362.46	-5.52	5.19	1.17 (0.04)
Ibuprofen	3.20	206.28	-0.24	22.08	7.28 (0.27)

Indomethacin	4.04	357.79	-1.30	16.61	3.57 (0.16)
Ketoprofen	2.23	254.28	-1.23	6.39	1.28 (0.07)
Lidocaine	3.01	234.34	-1.70 [35]	18.21	7.30 (0.21)
m-Cresol	2.09	108.14	-1.82	11.26	2.39 (0.07)
Methyl nicotinate	0.93	137.14	-2.49	2.75	2.08 (0.08)
Methyl-4-hydroxybenzoate	1.36	152.15	-2.04	10.10	1.50 (0.05)
m-Nitrophenol	2.21	139.11	-2.25	15.51	2.07 (0.06)
Naproxen	3.23	230.26	-1.42	10.61	2.29 (0.09)
o-Chlorophenol	2.40	128.56	-1.48	14.84	2.86 (0.08)
o-Cresol	2.07	108.14	-1.80	12.63	2.48 (0.08)
Paracetamol	1.07	151.16	-3.35	1.08	0.16 (0.03)
p-Cresol	2.16	108.14	-0.92	11.09	2.44 (0.08)
Phenobarbitone	1.49	232.24	-3.35	6.40	1.67 (0.05)
Phenol	1.59	94.11	-1.71	6.70	1.35 (0.04)
Piroxicam	1.59	331.35	-2.47	4.64	1.14 (0.06)
p-Nitrophenol	2.17	139.11	-2.25	13.34	1.84 (0.06)
p-Phenylenediamine	0.23	108.14	-3.62	4.57	1.44 (0.06)
Prednisolone	-0.45	360.44	-4.35	5.44	1.33 (0.11)
Progesterone	2.85	314.46	-2.82	19.12	6.55 (0.19)
Resorcinol	1.18	110.11	-3.62	1.97	0.34 (0.03)
Salicylic acid	0.96	138.12	-2.20	0.45	0.05 (0.03)
Testosterone	2.48	288.42	-3.40	12.06	2.58 (0.09)
Thiourea	-0.65	76.12	-4.02 [32]	0.69	0.12 (0.03)
Thymol	3.23	150.22	-1.28	38.94	7.34 (0.20)
Triamcinolone	-1.13	394.43	-5.40	3.53	0.58 (0.03)
Triamcinolone acetonide	1.40	434.50	-4.69	11.44	2.11 (0.07)
β-estradiol	3.37	272.38	-2.37	29.57	1.65 (0.07)
β-naphthol	2.61	144.17	-1.55	23.12	4.43 (0.13)

417 [a] (Virtual) log *P* and *MW* [g.mol^{-1}] were calculated with Vega ZZ software.

418 [b] The log K_p values [cm.h^{-1}] were mostly obtained from a validated database [31]. Other sources are

419 indicated.

420 **Table 4.** The best MLR models containing the (logarithm of the) retention factors obtained on the particle-based column ($k_{particle}$), along with the standard error
421 on the coefficients, together with their root mean squared error of calibration (RMSEC), root mean squared error of cross validation (RMSECV), both with their
422 relative values (calculated using the average log K_p value), and the determination coefficient (r^2) values.

RMSEC	**RMSECV**	r^2	***n***	**Equation**
0.675 (25.3%)	0.733 (27.5%)	0.71	57	log K_p = -2.36(±0.29) – 0.20(±0.33) log $k_{particle}$ – 0.026(±0.009) *Atoms* + 0.64(±0.12) *Virtual log P* – 0.0040(±0.0019) *Melting point* (Eq. 2)
0.329 (12.4%)	0.399 (15.0%)	0.93	57	log K_p = -2.19(±0.44) – 0.36(±0.03) *RDF020e* + 0.51(±0.07) *C-025* + 0.66(±0.12) log $k_{particle}$ + 1.88(±0.31) *Lop* + 0.25(±0.05) *nCconj* – 1.45(±0.30) *GATS2p* + 0.78(±0.20) *Mor11m* – 6.68(±2.24) *RBF* – 1.01(±0.30) *G1p* – 7.68(±3.36) *JGI5* (Eq. 3)

423 Description of the selected E-Dragon descriptors: see **Table S3**.

Table 5. The best MLR models containing the (logarithm of) retention factor obtained on the monolithic column at flow rates of 1 mL/min (k_{m1}) and 8 mL/min (k_{m8}), along with the standard error on the coefficients, together with their performance parameters.

RMSEC	RMSECV	r^2	*n*	Equation
0.676 (25.4%)	0.735 (27.6%)	0.70	57	log K_p = -2.15(±0.35) + 0.17(±0.28) log k_{m1} – 0.040(±0.007) *Atoms* + 0.52(±0.11) *Virtual log P* – 0.20(±0.10) *HbDon* (Eq. 4)
0.670 (25.0%)	0.734 (27.4%)	0.72	55	log K_p = -2.18(±0.36) + 0.46(±0.33) log k_{m8} – 0.041(±0.007) *Atoms* + 0.47(±0.12) *Virtual log P* – 0.18(±0.11) *HbDon* (Eq. 5)
0.345 (13.0%)	0.425 (16.0%)	0.92	57	log K_p = -8.26(±1.96) – 0.40(±0.03) *RDF020e* + 0.43(±0.07) *C-025* + 0.13(±0.03) k_{m1} – 0.98(±0.27) *G1u* + 11.37(±2.46) *JGI4* – 1.65(±0.42) *GATS2e* + 1.20(±0.23) *Lop* + 1.69(±0.49) *BEHm1* + 0.88(±0.37) *MATS3m* + 0.17(±0.07) *EEig11d* (Eq. 6)
0.342 (12.8%)	0.408 (15.3%)	0.92	57	log K_p = -1.83(±0.41) – 0.42(±0.03) *RDF020e* + 0.36(±0.08) *C-025* + 0.85(±0.13) log k_{m1} – 0.96(±0.28) *G1u* + 2.22(±0.35) *Lop* + 0.20(±0.07) *EEig11d* – 9.75(±2.30) *RBF* – 1.81(±0.48) *GATS2e* – 1.28(±0.31) *Mor18m* + 23.03(±11.16) *JGI8* (Eq. 7)
0.377 (14.2%)	0.459 (17.2%)	0.91	57	log K_p = -0.86(±0.38) – 0.23(±0.03) *RDF020e* + 0.40(±0.07) *C-025* + 0.12(±0.03) k_{m8} – 1.20(±0.31) *G1u* – 2.17(±0.55) *GATS2p* – 1.89(±0.46) *E2s* – 0.20(±0.05) *nCs* + 0.054(±0.017) *H-046* + 1.59(±0.59) *GATS2m* (Eq. 8)
0.337 (12.6%)	0.412 (15.4%)	0.93	55	log K_p = -3.33(±0.38) – 0.35(±0.03) *RDF020e* + 0.39(±0.07) *C-025* + 0.80(±0.17) log k_{m8} – 0.86(±0.30) *G1u* + 2.21(±0.35) *Lop* + 0.21(±0.07) *EEig11d* – 0.14(±0.06) *ALOGPS_logS* + 0.56(±0.21) *Mor11m* – 13.25(±2.83) *RBF* + 1.67(±0.58) *MATS2e* – 0.61(±0.29) *Mor18m* (Eq. 9)

Description of the selected E-Dragon descriptors: see **Table S3**.

Figures

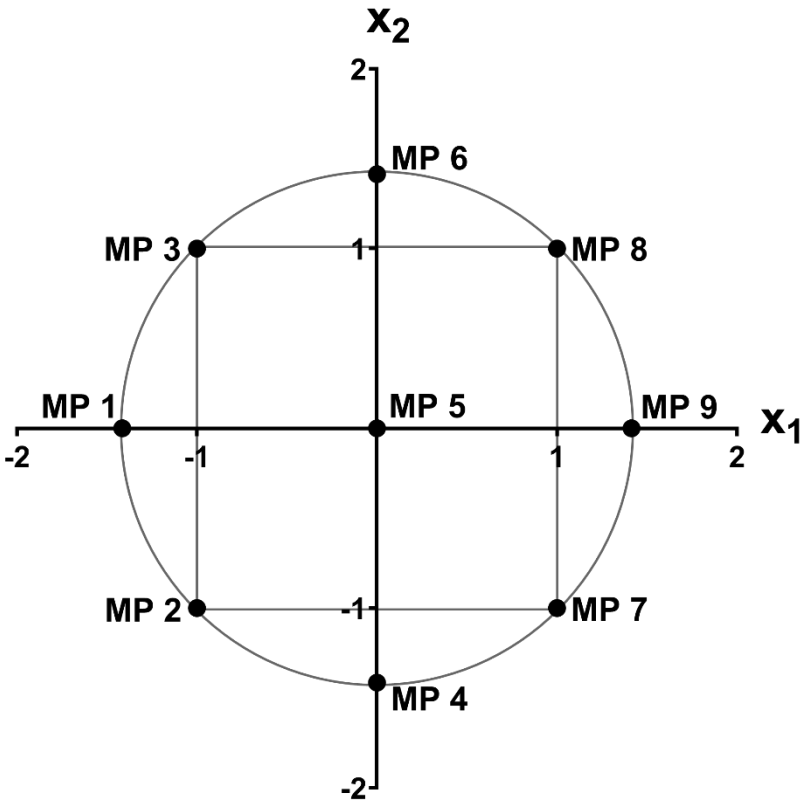

Fig. 1. Visual representation of the two-factor central composite design to optimize the concentration of SDS (x_1) and the fraction of 1-propanol (x_2) in the mobile phase. The labelled dots indicate the nine tested mobile-phase (MP) compositions. The levels are defined in **Table 1**.

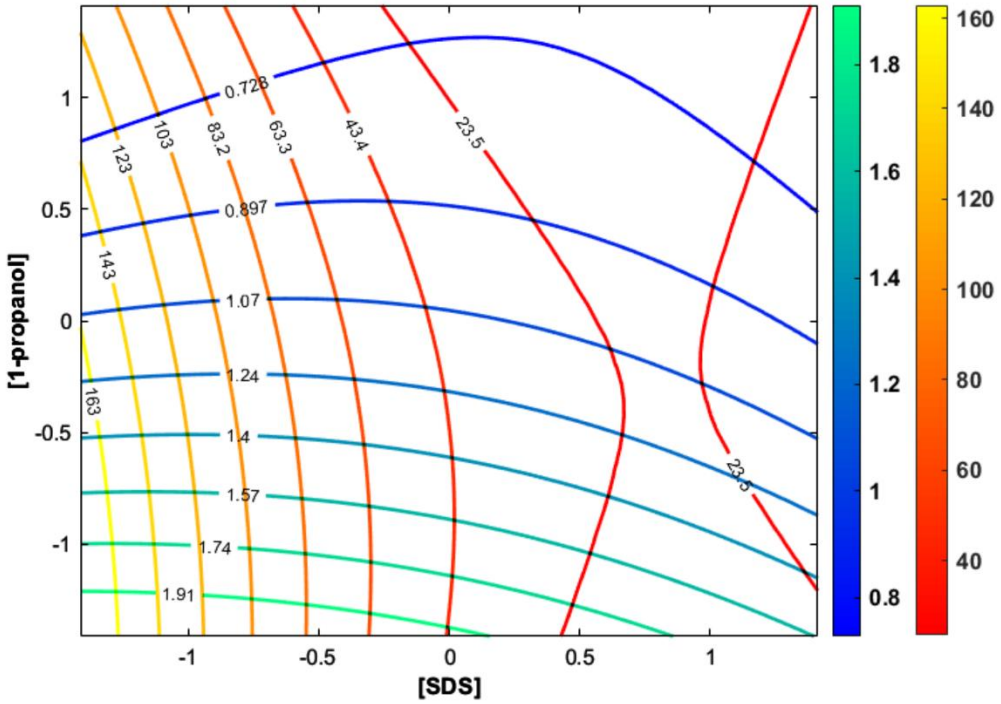

Fig. 2. Overlay of the contour plots for the predicted retention factors of caffeine (horizontal lines in blue/green) and thymol (vertical lines in red/yellow).

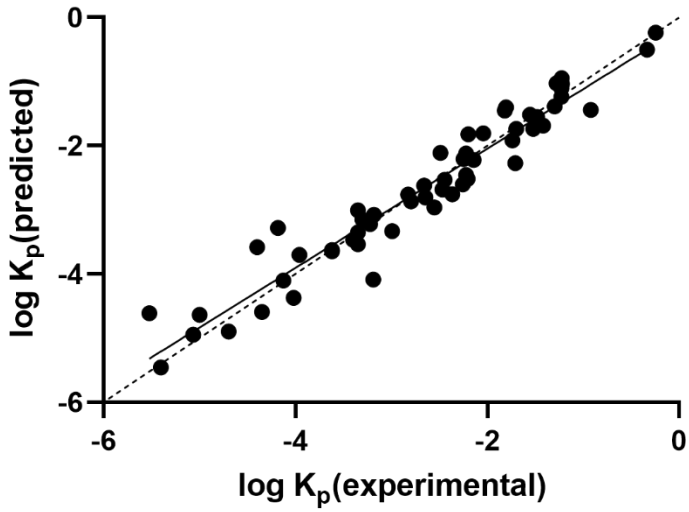

Fig. 3. The predicted skin permeability coefficients log K_p, based on the results from the stepwise MLR model, including the log $k_{particle}$ and E-Dragon descriptors (Eq. 3), versus the experimental values, together with the regression line (solid line) and the bisector (y = x, dashed line).

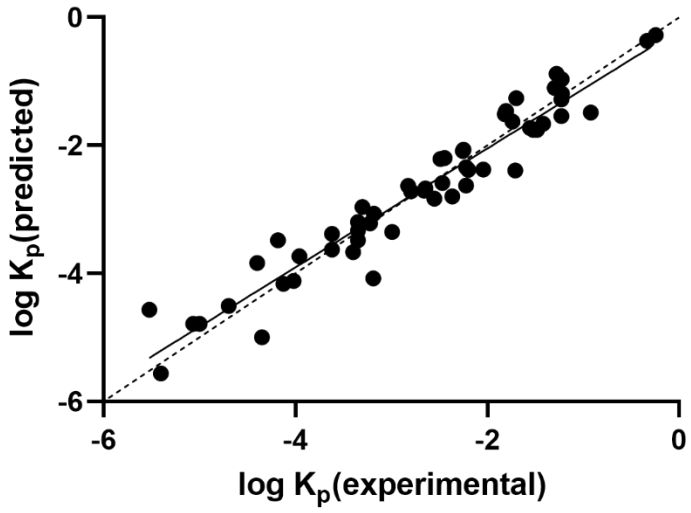

439

440 **Fig. 4.** The predicted log K_p values from the stepwise MLR model containing the log k_{m8} on the
441 monolithic column and E-Dragon descriptors (Eq. 9), versus the experimental. The regression line (solid
442 line) and bisector (dashed line) are also shown.

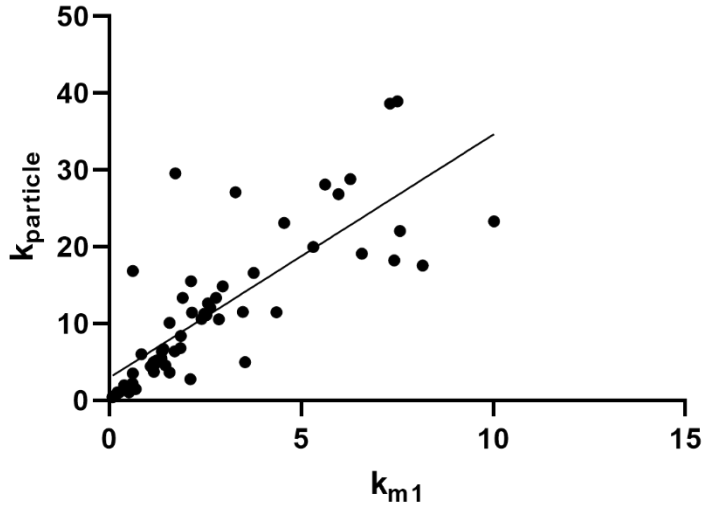

443

444 **Fig. 5.** The retention factors (without haloperidol) obtained on the particle column ($k_{particle}$) versus the
445 retention factors on the monolithic column (k_{m1}), together with the regression line.

References

[1] J. Kielhorn, S. Melching-Kollmuß, I. Mangelsdorf, Environmental Health Criteria 235: Dermal Absorption, World Health Organization Press, Geneva, 2006.

[2] R. Neupane, S.H.S. Boddu, J. Renukuntla, R.J. Babu, A.K. Tiwari, Alternatives to biological skin in permeation studies: current trends and possibilities, Pharmaceutics. 12 (2020) 152. https://doi.org/10.3390/PHARMACEUTICS12020152.

[3] F. Barbato, B. Cappello, A. Miro, M.I. La Rotonda, F. Quaglia, Chromatographic indexes on immobilized artificial membranes for the prediction of transdermal transport of drugs, Il Farmaco. 53 (1998) 655–661. https://doi.org/10.1016/S0014-827X(98)00082-2.

[4] A. Nasal, M. Sznitowska, A. Buciński, R. Kaliszan, Hydrophobicity parameter from high-performance liquid chromatography on an immobilized artificial membrane column and its relationship to bioactivity, J. Chromatogr. A. 692 (1995) 83–89. https://doi.org/10.1016/0021-9673(94)00689-7.

[5] M. Turowski, R. Kaliszan, Keratin immobilized on silica as a new stationary phase for chromatographic modelling of skin permeation, J. Pharm. Biomed. Anal. 15 (1997) 1325–1333. https://doi.org/10.1016/S0731-7085(96)02009-2.

[6] Y. Wang, J. Sun, H. Liu, J. Liu, L. Zhang, K. Liu, Z. He, Predicting skin permeability using liposome electrokinetic chromatography, Analyst. 134 (2009) 267–272. https://doi.org/10.1039/b807497f.

[7] M. Turowski, R. Kaliszan, Collagen immobilised on silica derivatives as a new stationary phase for HPLC, Biomed. Chromatogr. 12 (1998) 187–192. https://doi.org/10.1002/(SICI)1099-0801(199807/08)12:4<187::AID-BMC727>3.0.CO;2-2.

[8] E. Lázaro, C. Ràfols, M.H. Abraham, M. Rosés, Chromatographic estimation of drug disposition properties by means of immobilized artificial membranes (IAM) and C18 columns, J. Med. Chem. 49 (2006) 4861–4870. https://doi.org/10.1021/jm0602108.

[9] M. Hidalgo-Rodríguez, S. Soriano-Meseguer, E. Fuguet, C. Ràfols, M. Rosés, Evaluation of the suitability of chromatographic systems to predict human skin permeation of neutral compounds, Eur. J. Pharm. Sci. 50 (2013) 557–568. https://doi.org/10.1016/j.ejps.2013.04.005.

[10] Y. Grooten, A. Sych, D. Mangelings, Y. Vander Heyden, Comparison of in-silico modelling and reversed-phase liquid chromatographic retention on an octadecyl silica column to predict skin permeability of pharmaceutical and cosmetic compounds, J. Pharm. Biomed. Anal. 201 (2021) 114095. https://doi.org/10.1016/j.jpba.2021.114095.

[11] S. Soriano-Meseguer, E. Fuguet, A. Port, M. Rosés, Estimation of skin permeation by liquid chromatography, ADMET DMPK. 6 (2018) 140–152. https://doi.org/10.5599/admet.512.

[12] A.W. Sobańska, J. Robertson, E. Brzezińska, Application of RP-18 TLC retention data to the prediction of the transdermal absorption of drugs, Pharmaceuticals. 14 (2021) 147. https://doi.org/10.3390/PH14020147.

[13] M.J. Ruiz-Ángel, S. Carda-Broch, J.R. Torres-Lapasió, M.C. García-Álvarez-Coque, Retention mechanisms in micellar liquid chromatography, J. Chromatogr. A. 1216 (2009) 1798–1814. https://doi.org/10.1016/j.chroma.2008.09.053.

[14] M.C. García-Alvarez-Coque, M.J. Ruiz-Angel, E. Peris-García, Liquid Chromatography | Micellar Liquid Chromatography, in: P. Worsfold, A. Townshend, C. Poole, M. Miró (Eds.), Encyclopedia of Analytical Science, third ed., Elsevier, Amsterdam, The Netherlands, 2019, pp. 133–142.

[15] L. Escuder-Gilabert, J.J. Martínez-Pla, S. Sagrado, R.M. Villanueva-Camañas, M.J. Medina-Hernández, Biopartitioning micellar separation methods: modelling drug absorption, J. Chromatogr. B. 797 (2003) 21–35. https://doi.org/10.1016/S1570-0232(03)00606-8.

[16] C.F. Poole, The Column in Liquid Chromatography, in: The Essence of Chromatography, Elsevier Science, Amsterdam, The Netherlands, 2003, pp. 267–429.

[17] R.N. El-Shaheny, M.H. El-Maghrabey, F.F. Belal, Micellar liquid chromatography from green analysis perspective, Open Chem. 13 (2015) 877–892. https://doi.org/10.1515/chem-2015-0101.

[18] L.J. Waters, Y. Shahzad, J. Stephenson, Modelling skin permeability with micellar liquid chromatography, Eur. J. Pharm. Sci. 50 (2013) 335–340. https://doi.org/10.1016/j.ejps.2013.08.002.

[19] J.J. Martínez-Pla, Y. Martín-Biosca, S. Sagrado, R.M. Villanueva-Camañas, M.J. Medina-Hernández, Biopartitioning micellar chromatography to predict skin permeability, Biomed. Chromatogr. 17 (2003) 530–537. https://doi.org/10.1002/bmc.281.

[20] J.J. Martínez-Pla, Y. Martín-Biosca, S. Sagrado, R.M. Villanueva-Camañas, M.J. Medina-Hernández, Evaluation of the pH effect of formulations on the skin permeability of drugs by biopartitioning micellar chromatography, J. Chromatogr. A. 1047 (2004) 255–262. https://doi.org/10.1016/j.chroma.2004.07.011.

[21] V. Dobričić, K. Nikolic, S. Vladimirov, O. Čudina, Biopartitioning micellar chromatography as a predictive tool for skin and corneal permeability of newly synthesized 17β-carboxamide steroids, Eur. J. Pharm. Sci. 56 (2014) 105–112. https://doi.org/10.1016/j.ejps.2014.02.007.

[22] G. Guiochon, Monolithic columns in high-performance liquid chromatography, J. Chromatogr. A. 1168 (2007) 101–168. https://doi.org/10.1016/j.chroma.2007.05.090.

[23] P.G. Wang, Monolithic Chromatography and its Modern Applications, first ed., ILM Publications, St Albans, UK, 2010.

[24] K. Cabrera, Applications of silica-based monolithic HPLC columns, J. Sep. Sci. 27 (2004) 843–852. https://doi.org/10.1002/jssc.200401827.

[25] A. Detroyer, Y. Vander Heyden, K. Reynaert, D.L. Massart, Evaluating “fast” micellar monolithic liquid chromatography for high-throughput quantitative structure-retention relationship screening, Anal. Chem. 76 (2004) 1903–1908. https://doi.org/10.1021/ac030339e.

519 [26] R. Lu, J. Sun, Y. Wang, H. Li, J. Liu, L. Fang, Z. He, Characterization of biopartitioning micellar
520 chromatography system using monolithic column by linear solvation energy relationship and
521 application to predict blood-brain barrier penetration, J. Chromatogr. A. 1216 (2009) 5190–5198.
522 https://doi.org/10.1016/j.chroma.2009.05.007.

523 [27] I. Rapado-Martínez, M.C. García-Alvarez-Coque, R.M. Villanueva-Camañas, Liquid
524 chromatographic procedure for the evaluation of β-blockers in pharmaceuticals using hybrid
525 micellar mobile phases, J. Chromatogr. A. 765 (1997) 221–231. https://doi.org/10.1016/S0021-
526 9673(96)00919-3.

527 [28] L.J. Waters, Y. Shahzad, J.C. Mitchell, pH effects in micellar liquid chromatographic analysis
528 for determining partition coefficients for a series of pharmaceutically related compounds, Curr.
529 Pharm. Anal. 8 (2012) 272–277. https://doi.org/10.2174/157341212801619379.

530 [29] A. Detroyer, Y. Vander Heyden, S. Carda-Broch, M.C. García-Alvarez-Coque, D.L. Massart,
531 Quantitative structure-retention and retention-activity relationships of β-blocking agents by
532 micellar liquid chromatography, J. Chromatogr. A. 912 (2001) 211–221.
533 https://doi.org/10.1016/s0021-9673(01)00577-5.

534 [30] M.J. Ruiz-Angel, R.D. Caballero, E.F. Simó-Alfonso, M.C. García-Alvarez-Coque, Micellar
535 liquid chromatography: suitable technique for screening analysis, J. Chromatogr. A. 947 (2002)
536 31–45. https://doi.org/10.1016/S0021-9673(01)01595-3.

537 [31] B.E. Vecchia, A.L. Bunge, Skin Absorption Databases and Predictive Equations, in: R.H. Guy,
538 J. Hadgraft (Eds.), Transdermal Drug Delivery, Marcel Dekker, New York, 2003, pp. 57–141.

539 [32] K.T. Hoang, Dermal Exposure Assessment: Principles and Applications, Environmental
540 Protection Agency, Office of Health and Environmental Assessment, EPA/600/8–91/011B,
541 Washington DC, USA, 1992.

542 [33] I.T. Degim, W.J. Pugh, J. Hadgraft, Skin permeability data: anomalous results, Int. J. Pharm. 170
543 (1998) 129–133. https://doi.org/10.1016/S0378-5173(98)00113-6.

[34] A.F. Azarbayjani, H. Lin, C.W. Yap, Y.W. Chan, S.Y. Chan, Surface tension and wettability in transdermal delivery: a study on the in-vitro permeation of haloperidol with cyclodextrin across human epidermis, J. Pharm. Pharmacol. 62 (2010) 770–778. https://doi.org/10.1211/jpp.62.06.0014.

[35] J. Thomas, S. Majumdar, S. Wasdo, A. Majumdar, K.B. Sloan, The effect of water solubility of solutes on their flux through human skin in vitro: an extended Flynn database fitted to the Roberts-Sloan equation, Int. J. Pharm. 339 (2007) 157–167. https://doi.org/10.1016/j.ijpharm.2007.02.031.

[36] A. Pedretti, L. Villa, G. Vistoli, VEGA - an open platform to develop chemo-bio-informatics applications, using plug-in architecture and script programming, J. Comput. Aided. Mol. Des. 18 (2004) 167–173. https://doi.org/10.1023/b:jcam.0000035186.90683.f2.

[37] S. Kim, J. Chen, T. Cheng, A. Gindulyte, J. He, S. He, Q. Li, B.A. Shoemaker, P.A. Thiessen, B. Yu, L. Zaslavsky, J. Zhang, E.E. Bolton, PubChem 2019 update: improved access to chemical data, Nucleic Acids Res. 47 (2019) D1102–D1109. https://doi.org/10.1093/nar/gky1033.

[38] I.V. Tetko, J. Gasteiger, R. Todeschini, A. Mauri, D. Livingstone, P. Ertl, V.A. Palyulin, E.V. Radchenko, N.S. Zefirov, A.S. Makarenko, V.Y. Tanchuk, V.V. Prokopenko, Virtual computational chemistry laboratory – design and description, J. Comput. Aided. Mol. Des. 19 (2005) 453–463. https://doi.org/10.1007/s10822-005-8694-y.

[39] I.V. Tetko, Computing chemistry on the web, Drug Discov. Today. 10 (2005) 1497–1500. https://doi.org/10.1016/S1359-6446(05)03584-1.